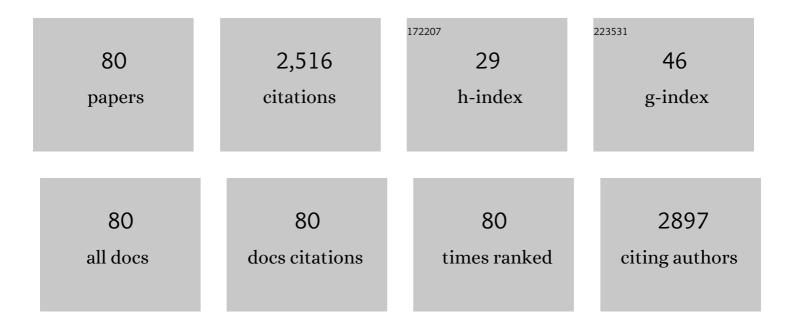
Masoud Torkzadeh-Mahani

List of Publications by Year in descending order

Source: https://exaly.com/author-pdf/4023067/publications.pdf Version: 2024-02-01



#	Article	lF	CITATIONS
1	New insight into the molecular mechanism of the trehalose effect on urate oxidase stability. Journal of Biomolecular Structure and Dynamics, 2022, 40, 1461-1471.	2.0	7
2	Silicon and nitric oxide synergistically modulate the production of essential oil and rosmarinic acid in Salvia officinalis under Cu stress. Protoplasma, 2022, 259, 905-916.	1.0	18
3	Carbon quantum dots—Annexin V probe: photoinduced electron transfer mechanism, phosphatidylserine detection, and apoptotic cell imaging. Mikrochimica Acta, 2022, 189, 69.	2.5	12
4	Effect of gamma-irradiation on electrochemical properties of ZnCo2O4-rGO for supercapacitor application. Diamond and Related Materials, 2022, 127, 109157.	1.8	8
5	Stabilization of recombinant d-Lactate dehydrogenase enzyme with trehalose: Response surface methodology and molecular dynamics simulation study. Process Biochemistry, 2021, 101, 26-35.	1.8	10
6	Niosomal virosome derived by vesicular stomatitis virus glycoprotein as a new gene carrier. Biochemical and Biophysical Research Communications, 2021, 534, 980-987.	1.0	21
7	Preparation and Characterization of ZnCo2O4 as a Binary Transitional Metal Oxide Towards Pseudocapacitor Electrode Materials. Brazilian Journal of Physics, 2021, 51, 420-428.	0.7	5
8	Polycaprolactone/gelatin electrospun nanofibres containing biologically produced tellurium nanoparticles as a potential wound dressing scaffold: Physicochemical, mechanical, and biological characterisation. IET Nanobiotechnology, 2021, 15, 277-290.	1.9	13
9	Bioactive anti-oxidative polycaprolactone/gelatin electrospun nanofibers containing selenium nanoparticles/vitamin E for wound dressing applications. Journal of Biomaterials Applications, 2021, 36, 193-209.	1.2	17
10	Improvement Thermal Stability of d-Lactate Dehydrogenase by Hydrophobin-1 and in Silico Prediction of Protein–Protein Interactions. Molecular Biotechnology, 2021, 63, 919-932.	1.3	1
11	Enhancement of Thermostability of Aspergillus flavus Urate Oxidase by Immobilization on the Ni-Based Magnetic Metal–Organic Framework. Nanomaterials, 2021, 11, 1759.	1.9	22
12	In Silico Analysis of Relative Rareness, Codon Usage, and Enzymesubstrate Docking of Lampyroidea Maculata luciferase. Current Proteomics, 2021, 18, 424-434.	0.1	0
13	Biosynthesis of spinel nickel ferrite nanowhiskers and their biomedical applications. Scientific Reports, 2021, 11, 17431.	1.6	53
14	Genome-wide identification and characterization of legume T2 Ribonuclease gene family and analysis of GmaRNS9, a soybean T2 Ribonuclease gene, function in nodulation. 3 Biotech, 2021, 11, 495.	1.1	3
15	In silico analysis of codon usage and rare codon clusters in the halophilic bacteria L-asparaginase. Biologia (Poland), 2020, 75, 151-160.	0.8	5
16	Bimetallic nickel-ferrite nanorod particles: greener synthesis using rosemary and its biomedical efficiency. Artificial Cells, Nanomedicine and Biotechnology, 2020, 48, 242-251.	1.9	49
17	The Blepharis persica seed hydroalcoholic extract synergistically enhances the apoptotic effect of doxorubicin in human colon cancer and gastric cancer cells. Molecular Biology Reports, 2020, 47, 843-853.	1.0	6
18	From in vitro to in silico: Modeling and recombinant production of DT-Diaphorase enzyme. International Journal of Biological Macromolecules, 2020, 143, 213-223.	3.6	7

#	Article	IF	CITATIONS
19	A combined theoretical and experimental study to improve the thermal stability of recombinant D″actate dehydrogenase immobilized on a novel superparamagnetic Fe ₃ O ₄ NPs@metal–organic framework. Applied Organometallic Chemistry, 2020, 34, e5581.	1.7	38
20	A new formulation of hydrophobin-coated niosome as a drug carrier to cancer cells. Materials Science and Engineering C, 2020, 113, 110975.	3.8	64
21	Comprehensive Evaluation of Gene Expression in Negative and Positive Trigger-based Targeting Niosomes in HEK-293 Cell Line. Iranian Journal of Pharmaceutical Research, 2020, 19, 166-180.	0.3	15
22	Electrochemical aptasensor for activated protein C using a gold nanoparticle – Chitosan/graphene paste modified carbon paste electrode. Bioelectrochemistry, 2019, 130, 107322.	2.4	16
23	The effect of different percentages of triethanolammonium butyrate ionic liquid on the structure and activity of urate oxidase: Molecular docking, molecular dynamics simulation, and experimental study. Journal of Molecular Liquids, 2019, 292, 111318.	2.3	35
24	A hydrophobin-based-biosensor layered by an immobilized lactate dehydrogenase enzyme for electrochemical determination of pyruvate. Bioelectrochemistry, 2019, 130, 107323.	2.4	14
25	Diosgenin-loaded niosome as an effective phytochemical nanocarrier: physicochemical characterization, loading efficiency, and cytotoxicity assay. DARU, Journal of Pharmaceutical Sciences, 2019, 27, 329-339.	0.9	48
26	Evaluation of Carum-loaded Niosomes on Breast Cancer Cells:Physicochemical Properties, In Vitro Cytotoxicity, Flow Cytometric, DNA Fragmentation and Cell Migration Assay. Scientific Reports, 2019, 9, 7139.	1.6	93
27	Electrochemical aptasensor for tumor necrosis factor α using aptamer–antibody sandwich structure and cobalt hexacyanoferrate for signal amplification. Journal of the Iranian Chemical Society, 2019, 16, 1783-1791.	1.2	18
28	In silico and in vitro study of magnetic niosomes for gene delivery: The effect of ergosterol and cholesterol. Materials Science and Engineering C, 2019, 94, 234-246.	3.8	73
29	<i>In vitro</i> cytotoxicity studies of parent and nanoencapsulated Holmium-2,9-dimethyl-1,10-phenanthroline complex toward fish-salmon DNA-binding properties and antibacterial activity. Journal of Biomolecular Structure and Dynamics, 2019, 37, 4437-4449.	2.0	14
30	Stabilization of d-lactate dehydrogenase diagnostic enzyme via immobilization on pristine and carboxyl-functionalized carbon nanotubes, a combined experimental and molecular dynamics simulation study. Archives of Biochemistry and Biophysics, 2019, 661, 178-186.	1.4	24
31	Synthesis and characterization of a novel organosilane-functionalized chitosan nanocarrier as an efficient gene delivery system: Expression of green fluorescent protein. International Journal of Biological Macromolecules, 2019, 125, 143-148.	3.6	8
32	Tris-chelated complexes of nickel(II) with bipyridine derivatives: DNA binding and cleavage, BSA binding, molecular docking, and cytotoxicity. Journal of Biomolecular Structure and Dynamics, 2019, 37, 3887-3904.	2.0	15
33	Controlled release of lawsone from polycaprolactone/gelatin electrospun nano fibers for skin tissue regeneration. International Journal of Biological Macromolecules, 2019, 124, 478-491.	3.6	118
34	In vitro cytotoxicity assay of D-limonene niosomes: an efficient nano-carrier for enhancing solubility of plant-extracted agents. Research in Pharmaceutical Sciences, 2019, 14, 448.	0.6	86
35	Application of antibody–nanogold–ionic liquid–carbon paste electrode for sensitive electrochemical immunoassay of thyroid-stimulating hormone. Biosensors and Bioelectronics, 2018, 110, 97-102.	5.3	87
36	Synthesis and characterization of aminotetrazole-functionalized magnetic chitosan nanocomposite as a novel nanocarrier for targeted gene delivery. Materials Science and Engineering C, 2018, 89, 166-174.	3.8	43

#	Article	IF	CITATIONS
37	MIAT lncRNA is overexpressed in breast cancer and its inhibition triggers senescence and G1 arrest in MCF7 cell line. Journal of Cellular Biochemistry, 2018, 119, 6470-6481.	1.2	67
38	Aptamer-based determination of tumor necrosis factor α using a screen-printed graphite electrode modified with gold hexacyanoferrate. Mikrochimica Acta, 2018, 185, 165.	2.5	22
39	Statistical optimization of kojic acid production by a UV-induced mutant strain of Aspergillus terreus. Brazilian Journal of Microbiology, 2018, 49, 865-871.	0.8	13
40	An Electrochemical Immunosensor Based on Poly(Thionine)-Modified Carbon Paste Electrode for the Determination of Prostate Specific Antigen. IEEE Sensors Journal, 2018, 18, 4861-4868.	2.4	11
41	Antixenosis and antibiosis response of common bean (Phaseolus vulgaris) to two-spotted spider mite (Tetranychus urticae). Experimental and Applied Acarology, 2018, 74, 365-381.	0.7	11
42	Evaluation of serum arsenic and its effects on antioxidant alterations in relapsing-remitting multiple sclerosis and Related Disorders, 2018, 19, 79-84.	0.9	30
43	Magnetic delivery of antitumor carboplatin by using PEGylated-Niosomes. DARU, Journal of Pharmaceutical Sciences, 2018, 26, 57-64.	0.9	66
44	Optimization of in vitro refolding conditions of recombinant Lepidium draba peroxidase using design of experiments. International Journal of Biological Macromolecules, 2018, 118, 1369-1376.	3.6	13
45	Improvement of kinetic properties and thermostability of recombinant Lepidium draba peroxidase (LDP) upon exposed to osmolytes. International Journal of Biological Macromolecules, 2018, 119, 1036-1041.	3.6	6
46	Double strand DNA-based determination of menadione using a Fe3O4 nanoparticle decorated reduced graphene oxide modified carbon paste electrode. Bioelectrochemistry, 2018, 124, 165-171.	2.4	11
47	Lawsone-loaded Niosome and its antitumor activity in MCF-7 breast Cancer cell line: a Nano-herbal treatment for Cancer. DARU, Journal of Pharmaceutical Sciences, 2018, 26, 11-17.	0.9	102
48	Amperometric immunosensor for prolactin hormone measurement using antibodies loaded on a nano-Au monolayer modified ionic liquid carbon paste electrode. Talanta, 2018, 188, 701-707.	2.9	43
49	Accumulation and phytoremediation of Pb, Zn, and Ag by plants growing on Koshk lead–zinc mining area, Iran. Journal of Soils and Sediments, 2017, 17, 1310-1320.	1.5	50
50	Electrochemical sandwich immunoassay for the prostate specific antigen using a polyclonal antibody conjugated to thionine and horseradish peroxidase. Mikrochimica Acta, 2017, 184, 2731-2738.	2.5	18
51	Heterologous Expression, Purification and Characterization of a Peroxidase Isolated from Lepidium draba. Protein Journal, 2017, 36, 461-471.	0.7	11
52	Evaluation of lithium serum level in multiple sclerosis patients: A neuroprotective element. Multiple Sclerosis and Related Disorders, 2017, 17, 244-248.	0.9	25
53	In vitro and in silico studies of the interaction of three tetrazoloquinazoline derivatives with DNA and BSA and their cytotoxicity activities against MCF-7, HT-29 and DPSC cell lines. International Journal of Biological Macromolecules, 2017, 94, 85-95.	3.6	46
54	Localized surface plasmon resonance based gold nanobiosensor: Determination of thyroid stimulating hormone. Analytical Biochemistry, 2017, 516, 1-5.	1.1	20

#	Article	IF	CITATIONS
55	Design of a Sensitive and Selective Electrochemical Aptasensor for the Determination of the Complementary cDNA of miRNA-145 Based on the Intercalation and Electrochemical Reduction of Doxorubicin. Journal of AOAC INTERNATIONAL, 2017, 100, 1754-1760.	0.7	4
56	Voltammetric determination of 6-thioguanine and folic acid using a carbon paste electrode modified with ZnO-CuO nanoplates and modifier. Materials Science and Engineering C, 2016, 69, 128-133.	3.8	68
57	Synthesis, characterization, crystal structure, DNA and BSA binding, molecular docking and in vitro anticancer activities of a mononuclear dioxido-uranium(VI) complex derived from a tridentate ONO aroylhydrazone. Journal of Photochemistry and Photobiology B: Biology, 2016, 158, 219-227.	1.7	41
58	A selective and regenerable voltammetric aptasensor for determination of homocysteine. Mikrochimica Acta, 2016, 183, 2205-2210.	2.5	16
59	Synthesis, crystal structure and Hirshfeld surface analysis of copper(II) complexes: DNA- and BSA-binding, molecular modeling, cell imaging and cytotoxicity. Polyhedron, 2016, 119, 23-38.	1.0	21
60	A magnetic core–shell Fe ₃ O ₄ @SiO ₂ /MWCNT nanocomposite modified carbon paste electrode for amplified electrochemical sensing of amlodipine and hydrochlorothiazide. Analytical Methods, 2016, 8, 6185-6193.	1.3	63
61	Competitive DNA-Binding Studies between Metal Complexes and GelRed as a New and Safe Fluorescent DNA Dye. Journal of Fluorescence, 2016, 26, 1505-1510.	1.3	19
62	Hydrophobinâ€1 promotes thermostability of firefly luciferase. FEBS Journal, 2016, 283, 2494-2507.	2.2	13
63	Sonochemical Synthesis and Characterization of the Copper(II) Nanocomplex: DNA- and BSA-Binding, Cell Imaging, and Cytotoxicity Against the Human Carcinoma Cell Lines. Journal of Fluorescence, 2016, 26, 545-558.	1.3	10
64	The Zn(II) nanocomplex: Sonochemical synthesis, characterization, DNA- and BSA-binding, cell imaging, and cytotoxicity against the human carcinoma cell lines. Journal of Fluorescence, 2016, 26, 1007-1020.	1.3	5
65	Development of a localized surface plasmon resonance-based gold nanobiosensor for the determination of prolactin hormone in human serum. Analytical Biochemistry, 2016, 495, 32-36.	1.1	25
66	Identification and characterization of a cathepsin L-like cysteine protease from Rhipicephalus (Boophilus) annulatus. Experimental and Applied Acarology, 2016, 68, 251-265.	0.7	11
67	Cadmium sulfide quantum dots modified with the human transferrin protein siderophiline for targeted imaging of breast cancer cells. Mikrochimica Acta, 2016, 183, 67-71.	2.5	22
68	Heterologous expression of a hydrophobin HFB1 and evaluation of its contribution to producing stable foam. Protein Expression and Purification, 2016, 118, 25-30.	0.6	19
69	In vitro DNA and BSA-binding, cell imaging and anticancer activity against human carcinoma cell lines of mixed ligand copper(II) complexes. Spectrochimica Acta - Part A: Molecular and Biomolecular Spectroscopy, 2015, 150, 390-402.	2.0	35
70	A mononuclear diketone-based oxido-vanadium(<scp>iv</scp>) complex: structure, DNA and BSA binding, molecular docking and anticancer activities against MCF-7, HPG-2, and HT-29 cell lines. RSC Advances, 2015, 5, 101063-101075.	1.7	52
71	Synthesis, characterization, X-ray crystal structure, DFT calculation, DNA binding, and antimicrobial assays of two new mixed-ligand copper(II) complexes. Spectrochimica Acta - Part A: Molecular and Biomolecular Spectroscopy, 2015, 142, 410-422.	2.0	57
72	Spectroscopic and electrochemical studies of the interaction between oleuropein, the major bio-phenol in olives, and salmon sperm DNA. Spectrochimica Acta - Part A: Molecular and Biomolecular Spectroscopy, 2015, 148, 260-265.	2.0	14

#	Article	IF	CITATIONS
73	Electrochemical determination of hydrochlorothiazide and folic acid in real samples using a modified graphene oxide sheet paste electrode. Materials Science and Engineering C, 2015, 52, 297-305.	3.8	50
74	A mononuclear Cu(II) complex with 5,6-diphenyl-3-(2-pyridyl)-1,2,4-triazine: Synthesis, crystal structure, DNA- and BSA-binding, molecular modeling, and anticancer activity against MCF-7, A-549, and HT-29 cell lines. European Journal of Medicinal Chemistry, 2015, 96, 66-82.	2.6	81
75	A Novel Strategy for Simultaneous Determination of Dopamine and Uric Acid Using a Carbon Paste Electrode Modified with CdTe Quantum Dots. Electroanalysis, 2015, 27, 524-533.	1.5	39
76	A mononuclear Ni(II) complex with 5,6-diphenyl-3-(2-pyridyl)-1,2,4-triazine: DNA- and BSA-binding and anticancer activity against human breast carcinoma cells. Spectrochimica Acta - Part A: Molecular and Biomolecular Spectroscopy, 2015, 136, 205-215.	2.0	44
77	Electrochemical determination of biophenol oleuropein using a simple label-free DNA biosensor. Bioelectrochemistry, 2015, 101, 52-57.	2.4	26
78	DNA- and BSA-binding studies and anticancer activity against human breast cancer cells (MCF-7) of the zinc(II) complex coordinated by 5,6-diphenyl-3-(2-pyridyl)-1,2,4-triazine. Spectrochimica Acta - Part A: Molecular and Biomolecular Spectroscopy, 2014, 127, 511-520.	2.0	117
79	Voltammetric behavior of uric acid on carbon paste electrode modified with salmon sperm dsDNA and its application as label-free electrochemical sensor. Biosensors and Bioelectronics, 2014, 54, 211-216.	5.3	28
80	Green and eco-friendly synthesis of silver nanoparticles by <i>Quercus infectoria</i> galls extract: thermal behavior, antibacterial, antioxidant and anticancer properties. Particulate Science and Technology, 0, , 1-9.	1.1	5